HARBOUR RESONANCE UNDER IMPACT OF POWERFUL TSUNAMI

Shentong Lu[1], Jiin-Jen Lee[2], and Xiuying Xing[3]

The powerful tsunami events caused by Feb. 27th, 2010 Chilean earthquake and Mar. 11th, 2011 Tohoku earthquake lead to the revelation of influence of tide level change in harbour oscillation. During a long time span of harbour excitement, the ocean surface will shift up and down, which, through dispersion relationship, makes the primary resonant mode to appear in various resonant spikes in the spectral density distribution. For the time domain analysis, the present paper uses the numerical model of the improved formula of Peregrine's Boussinesq-type equations to study the oscillation properties of three harbours in California with five representative tide levels. By white-noise analysis, the result of present paper in time domain is cross checked with earlier studies in frequency domain, and the effect of fluctuating tide level and the corresponding change of harbour layout is ascertained.

Keywords: harbour oscillation; resonant mode; tide level; harbour layout; Crescent City harbour

INTRODUCTION

Long waves can excite water body in the harbour area to slosh, as the period of incoming waves approach to the fundamental resonant mode. The rapid upward and downward movements of sea water can severely damage the vessels and mooring systems, especially when the sloshing frequency is close to the fundamental frequency of these attached facilities in harbours. Therefore, plenty of earlier studies have been devoted on simulating harbour oscillation based on frequency domain. A frequency domain study by Lee, Huang, Kou and Xing (2012) has found that during powerful tsunamis, such as the February 27th, 2010 Chilean tsunami and the March 11th, 2011 Tohoku tsunami, the Crescent City harbour in Northern California responded in a very different manner when compared with prior tsunami events as shown in Lee, Xing and Magoon (2008). As in Figure 1, the spectral analysis of the recorded water level at the tide gauge station revealed many resonant peaks between $2\times10^{-4}Hz$ and $10\times10^{-4}Hz$.

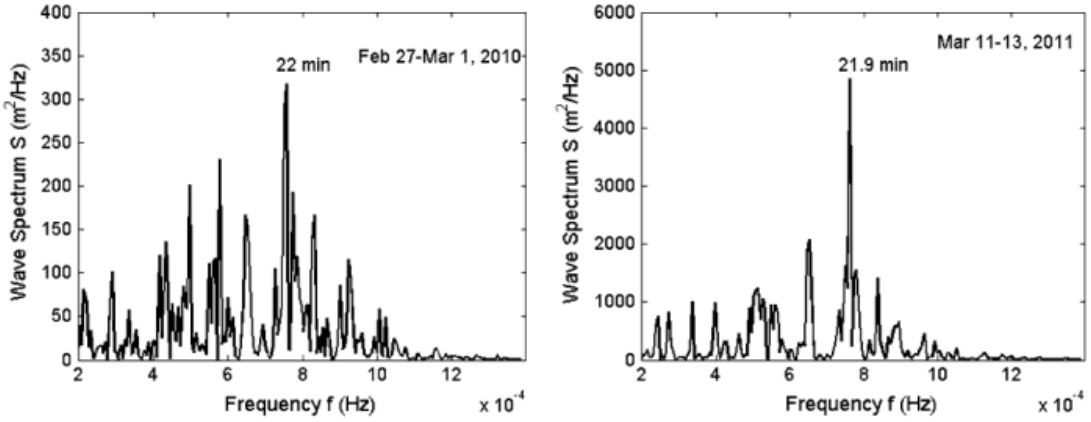

Figure 1. Spectral density distribution in Crescent City harbour during large tsunamis in 2010 and 2011 (Lee, Huang, Kou and Xing 2012).

They showed, by using dispersion relationship, the various resonant peaks are the manifestation of the fundamental resonant modes associated with the changing water depth because of extreme tide level changes. During the February 27th, 2010 Chilean earthquake tsunami, the tide level at the tide gauge station inside the Crescent City harbor varied from low tide at 0.6 m to high tide at 3.9 m. During the March 11th, 2011 Tohoku earthquake tsunami, the tide level at tide gauge station inside Crescent City harbor varied from 1.4 m at low tide to 3.1 m at high tide.

[1] Department of Civil and Environmental Engineering, University of Southern California, 3620 South Vermont Avenue, Los Angeles, CA, 90089, USA
[2] Department of Civil and Environmental Engineering, University of Southern California, 3620 South Vermont Avenue, Los Angeles, CA, 90089, USA
[3] Moffat & Nichol Engineers, 3780 Kilroy Airport Way, Long Beach, CA, 90808, USA

In this paper, the results of the frequency domain simulation are cross checked with the results of time domain simulation in Crescent City harbor of California to ascertain the effect of fluctuating tide level and the corresponding change of harbor layout on harbor resonance under the impact of powerful tsunami.

NUMERICAL MODEL

The numerical code of Mike21 developed by DHI is adopted, and it is based on the Boussinesq-type equations originally derived by Peregrine (1967):

$$\eta_t + P_x + Q_y = 0 \tag{1}$$

$$P_t + (\frac{P^2}{h})_x + (\frac{PQ}{h})_y + gh\eta_x + \psi_1 = 0 \tag{2}$$

$$Q_t + (\frac{Q^2}{h})_y + (\frac{PQ}{h})_x + gh\eta_y + \psi_2 = 0 \tag{3}$$

In the above equations, η is water surface elevation, h_0 is water depth at still, h is the total water surface elevation ($h=h_0+\eta$), P is the volume flux density in x direction ($P=uh$), Q is the volume flux density in y direction ($Q=vh$). The nonlinear Boussinesq terms ψ_1 and ψ_2 are defined by Madsen and Sorensen (1992) as follow:

$$\begin{aligned}\psi_1 = &-(B+\frac{1}{3})h_0^2(P_{xxt}+Q_{xyt}) - Bgh_0^3(\eta_{xxx}+\eta_{xyy}) \\ &- h_0(h_0)_x(\frac{1}{3}P_{xt}+\frac{1}{6}Q_{yt}+2Bgh_0\eta_{xx}+Bgh_0\eta_{yy}) \\ &- h_0(h_0)_y(\frac{1}{6}Q_{xt}+Bgh_0\eta_{xy}) = 0\end{aligned} \tag{4}$$

$$\begin{aligned}\psi_2 = &-(B+\frac{1}{3})h_0^2(Q_{yyt}+P_{xyt}) - Bgh_0^3(\eta_{yyy}+\eta_{xxy}) \\ &- h_0(h_0)_y(\frac{1}{3}Q_{yt}+\frac{1}{6}P_{xt}+2Bgh_0\eta_{yy}+Bgh_0\eta_{xx}) \\ &- h_0(h_0)_x(\frac{1}{6}P_{yt}+Bgh_0\eta_{xy}) = 0\end{aligned} \tag{5}$$

The time domain analysis conducted for the present study is based on the Boussinesq equation where nonlinearity and dispersion are equally important. The present numerical model uses Finite Difference (FD) method to numerically solve the governing equations (1) ~ (5). In present model, the temporal derivatives are discretized by Alternative Direction implicit (ADI) scheme, whereas the spatial derivatives are taken as straightforward mid-centering approximation in linear terms, and treated with "side-feeding" technique in the nonlinear convective terms. The resulting linear algebraic equations become a tri-diagonal matrix system, which is solved by the Double Sweep algorithm. The ADI scheme saves the hassle of iteration by linearizing the nonlinear terms, and the Double Sweep algorithm optimize actions to efficiently solve the tri-diagonal matrix system. The relevant technical details and derivations are accessible in the DHI documentation.

Reflective boundary and absorbing boundary are set along the coastline and outfield ocean to numerically simulate breakwater, rock armor, beach, and infinite ocean. The analytical solution derived by Madsen (1983) is used to define reflective boundaries:

$$\alpha_R = | a_r | / a_i = \frac{|1-\varepsilon+(1+\varepsilon)e^{-i2\kappa w}|}{1+\varepsilon+(1-\varepsilon)e^{-i2\kappa w}} \tag{6}$$

$$\varepsilon = \frac{n}{\sqrt{1-if}} \tag{7}$$

$$\kappa = \frac{w}{\sqrt{gh}}\sqrt{1-if} \tag{8}$$

where α_R is the reflection coefficient, a_i is the incoming wave amplitude, a_r is the reflected wave amplitude, n is the porosity of the structure, w is the thickness of the structure, f is the friction factor which is assumed to be independent of x and t. Figure 2 shows the layout of Crescent City harbor at high tide as well as the boundary conditions pointed out by the green lines. The reflective boundaries are defined with different reflection ratio, which is determined by the properties of coastlines.

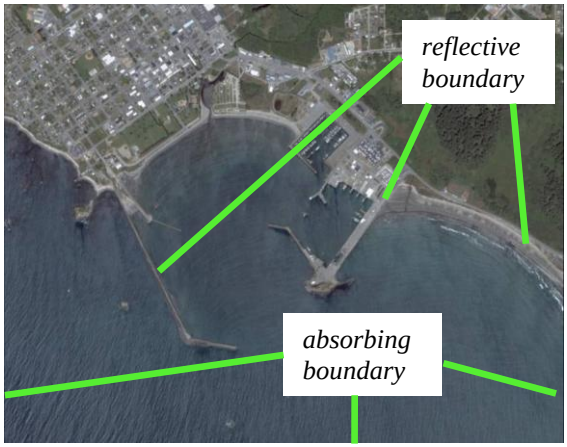

Figure 2. Air photo of Crescent City harbour with simulation boundary condition superimposed

The absorbing boundary adopts the formula provided by Larsen and Dancy (1983) to build a set of "sponge lines", which eliminates the radiated waves and flows. As travelling across sponge lines, the surface elevation and flow are weakened by the following division number:

$$\mu(x) = \begin{cases} \exp[(2^{-x/\Delta x} - 2^{-x_S/\Delta x})\ln a] & \text{for } 0 \le x \le x_s \\ 1 & \text{for } x_s < x \end{cases} \tag{9}$$

where, μ is the division number, x is location variable, x_s is the total thickness of the sponge layer, $\triangle x$ is the distance between two neighboring sponge lines, a is a constant number that is determined by the number of grid lines in the sponge layer.

CRESCENT CITY HARBOR

Ocean surface moves up and down within tidal cycles, which can change the layout of harbour. Figure 3 shows the layout of Crescent City harbour at water level of 0.8 m, 1.5 m, 2.3 m, 3.0 m, and 3.6 m (STDN) at the tide gauge station. The red part represents land, The blue part stands for sea water area, and the yellow part indicates the seabed that is exposed during low tide. The orange line marks the generation line of incoming waves from south, and the grey line denotes the generation boundary of incoming waves from west. The white star shows the location of tide gauge station, where field records are taken. The resolution is 9 m by 9 m, and there are 127,300 cells in the digital maps. The time step is 0.4 s, and courant number is 0.638.

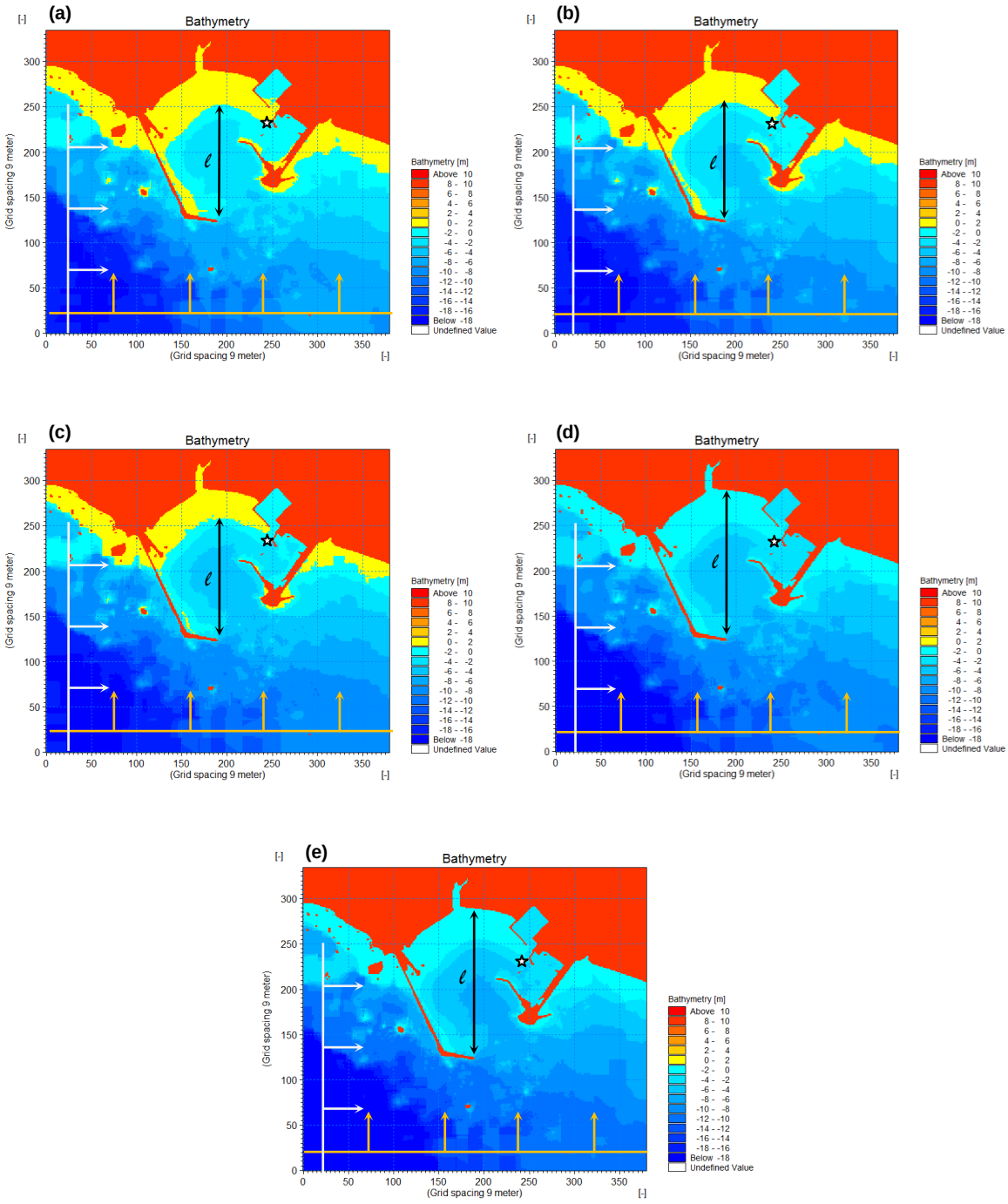

Figure 3. The layout and bathymetry of Crescent City harbour with water level of (a) 0.8 m; (b) 1.5 m; (c) 2.3 m; (d) 3.0 m; (e) 3.6 m at tide gauge station

In Figure 3, ℓ represents the characteristic length of Crescent City harbour, which is taken as the segment between the outer harbour entrance and the facing coastal line. As tide changes layout of the harbour, ℓ will be longer at high tide and shorter at low tide. Due to the changed bathymetry and layout of harbor, the primary resonant mode demonstrates different spikes in the spectral density distribution. In this paper, white-noise analysis is conducted and cross checked with the simulation results by mild-slope equation to further prove this hypothesis. The same set of waves trains are used as the incident waves, and their wave heights H are proportional to water depth at tide gauge station h_0 to remain a constant nonlinearity H/h_0.

Figure 4 shows the spectral result of white-noise analysis on Crescent City harbour on the five representative water levels at tide gauge station, which is marked as the white star in Figure 3.

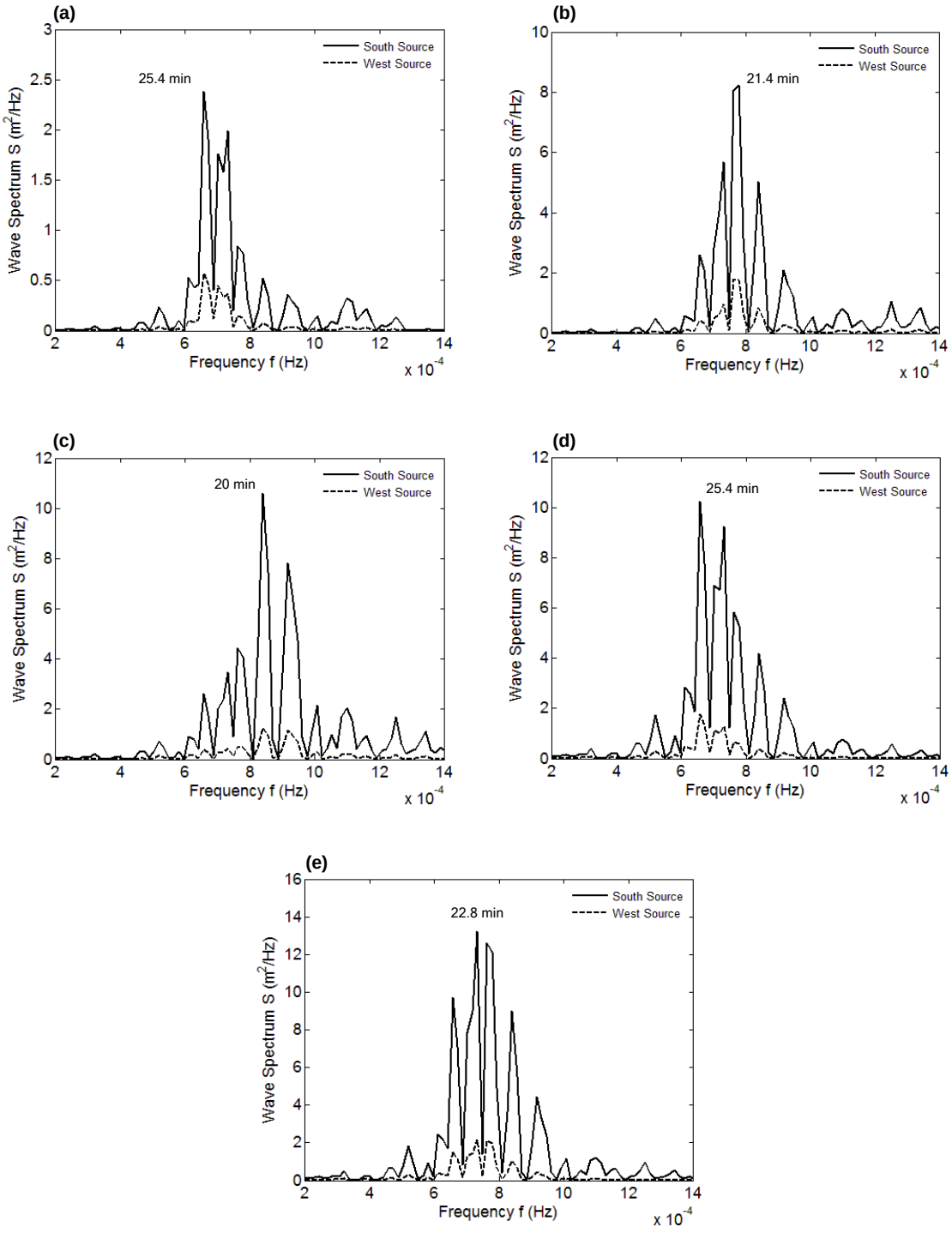

Figure 4. White-noise analysis results in Crescent City harbour with water level of (a) 0.8 m; (b) 1.5 m; (c) 2.3 m; (d) 3.0 m; (e) 3.6 m at tide gauge station

As shown in Figure 4, the primary resonant mode of Crescent City harbour is 25.4 min as water level is 0.8 m at tide gauge station, 21.4 min as water level is 1.5 m at tide gauge station, 20 min as water level is 2.3 m at tide gauge station, 25.4 min as water level is 3.0 m at tide gauge station, 22.8 min as water level is 3.6 m at tide gauge station.

Lee, Huang, Kou and Xing (2012) explain this phenomenon with dispersion relationship, and more evidences are needed to ascertain their study. Figure 5 demonstrates the response curves at the tide gauge station in Crescent City harbour, and the simulation is by mild-slope equation. In the dimensionless wave number $k\ell$, $k = 2\pi/L$ is the wave number. The L represents the characteristic wavelength of incoming waves, and ℓ stands for the characteristic length of harbor as shown in Figure 3. The amplification factor R is defined as ratio of wave amplitude at tidal gauge station to the amplitude of the incoming waves outside harbor.

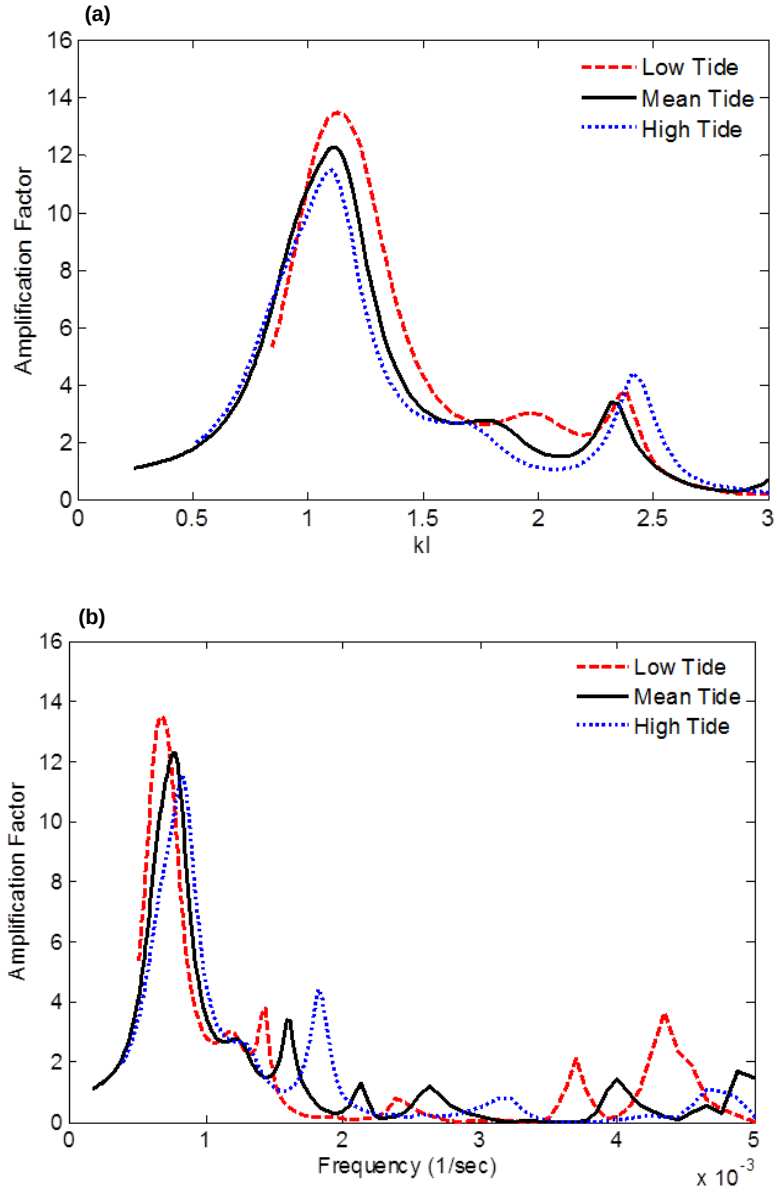

Figure 5. Response curves at tide gauge in Crescent City harbour with mean low water, mean tide level, and mean high water, based on station datum.

Figure 5 (a) indicates stable responses in Crescent City, because the three tide level yields a fairly consistent primary resonant mode with respect to the dimensionless wave number kl. Therefore, the characteristic length l can influence resonant mode to appear as different spikes with respect to frequency. In Figure 5 (b), the primary resonant modes appear to be 25 minutes at low tide, 22 minutes at mean tide, and 20 minutes at low tide. This result in frequency domain ascertains the influence of tide level and harbour layout on the oscillation response of Crescent City harbour to long waves.

So far, the analysis is based on separate tide levels, however, tide moves continuously in reality. To simulate this condition, the whole tide cycle is discretized into the five water levels shown in Figure 3, which take shift to represent the real tide fluctuation. The interval between water levels is 0.6 ~ 0.7 m, and this interval is enough to make the digital maps of Crescent City harbour evolve smoothly.

Figure 6 (a) shows the water level at tide gauge (Station Datum) in Crescent City harbour from Feb. 27th, 2010 to Mar. 3rd, 2010. Figure 6 (b) shows the water level at the same location from Mar. 11th, 2011 to Mar. 15th, 2011.

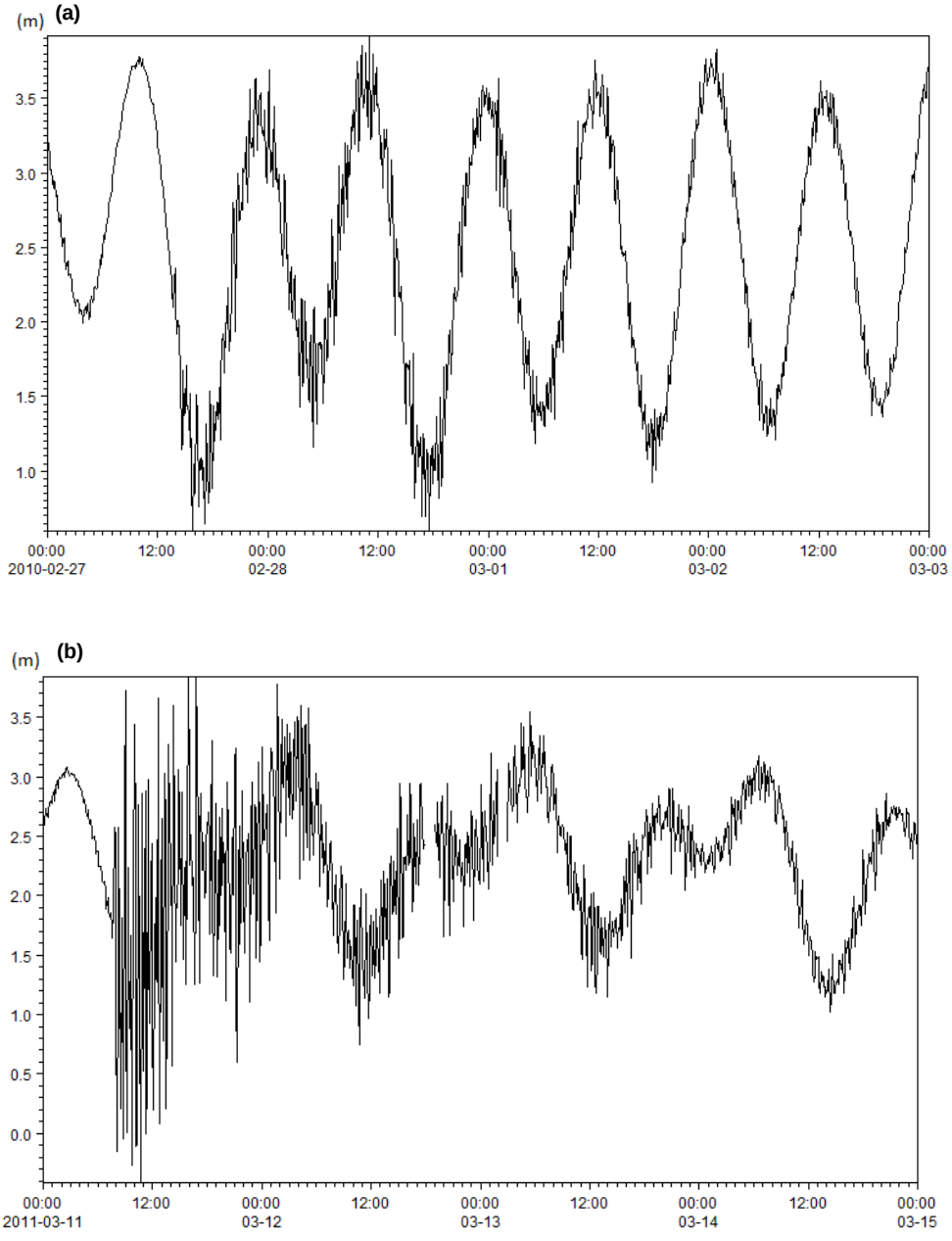

Figure 6. Water level at tide gauge (Station Datum) in Crescent City harbour (a) from Feb. 27th, 2010 to Mar. 3rd, 2010; (b) from Mar. 11th, 2011 to Mar. 15th, 2011 (Source: NOAA)

The tide level fluctuation makes harbour layout changes correspondingly, and different tide levels in Crescent City harbour have different primary resonant modes. The continuously moving tide level and the resulting change of harbour layout result in multiple resonant modes between 20 minutes and 25 minutes. To prove this, white-noise analysis is conducted with continuously switching tide levels and bathymetric maps to imitate the practical situation.

Figure 7 shows the spectral result of white-noise analysis on Crescent City harbour at tide gauge station, which is marked as the star in Figure 3. The fluctuating tide level and changing harbour layout are included in the simulation by Boussinesq model.

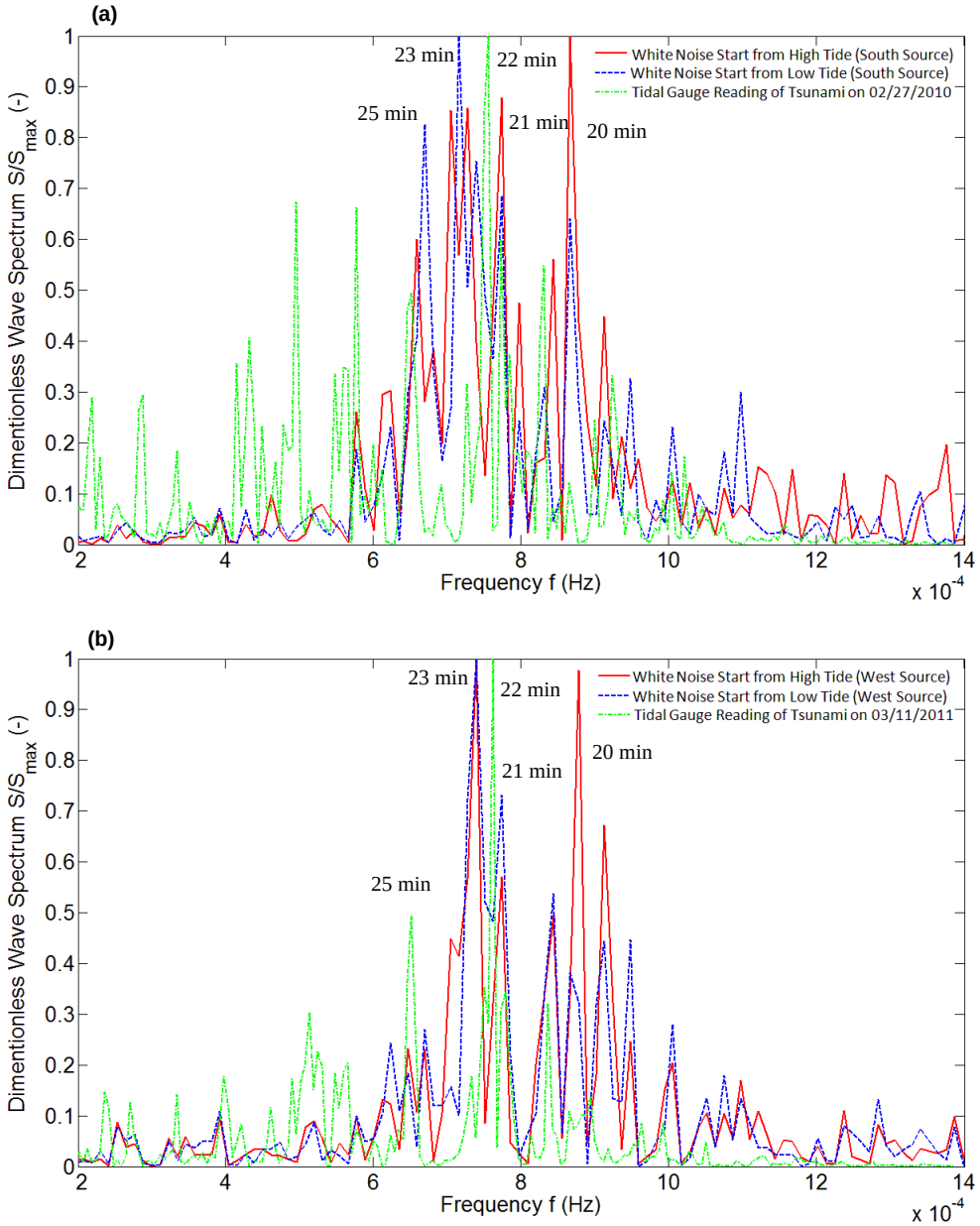

Figure 7. White-noise analysis at tide gauge compared with tide gauge records in Crescent City harbour with fluctuating tide level for (a) Feb. 27th, 2010 Chilean tsunami; (b) Mar. 11th, 2011 Tohoku tsunami

The red lines represent the spectrum of white-noise analysis with incident waves starting at high tide, and the blue lines represent the one of white-noise analysis with incoming waves starting at low tide. The tide gauge records of historical tsunami events are treated by FFT and shown as the green lines. (a) denotes the Feb. 27th, 2010 Chilean tsunami and south source simulations, and (b) demonstrates the Mar. 11th, 2011 Tohoku tsunami and west source simulations. By comparing the white-noise analysis and real tsunami oscillations, the multiple resonant modes between 20 min and 25 min are directly related to tide level fluctuation and the corresponding change of harbour layout. The multiple resonant modes are also observed on normal days with no tsunami influence. Xing, et al. (2010) and Lee, et al. (2012) analyze the spectral density distribution at tide gauge station on July 21st,

2008 (normal day), and the multiple resonant modes are compared with the ones on March 11th, 2011 (Tohoku tsunami), as shown in Figure 8.

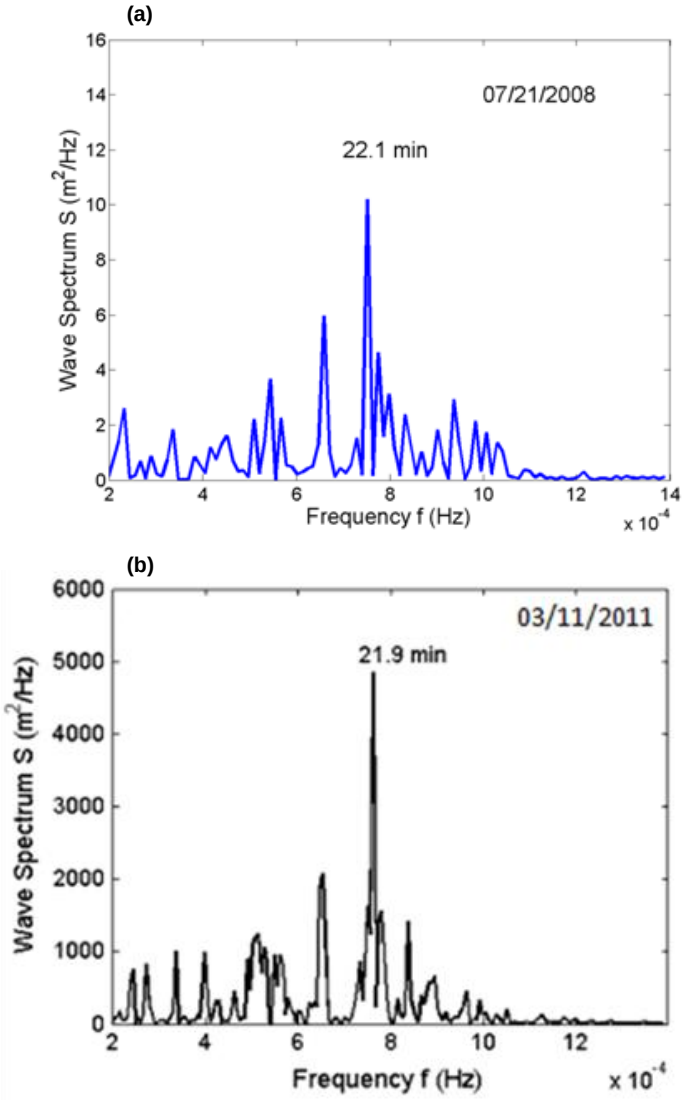

Figure 8. Wave Spectra at Tide Gauge Station in Crescent City on (a) Normal Day; (b) Tohoku tsunami (Xing, et al. 2010 and Lee, et al. 2012)

Figure 8, the profiles of spectra density distribution are fairly similar between normal day response and tsunami event response. The primary resonant mode is 22.1 minutes on July 21st, 2008, and 21.9 minutes on March 11th, 2011. The multiple spikes are observed in both charts, which provides Lee, et al. (2012) basis to prove that multiple resonant modes universally exist as the background energy content on normal days. Tsunami comes with bigger waves than regular long waves on normal days, and the difference in energy level is due to the wave amplitude.

The present paper investigates four representative normal days in 2013 in Crescent City harbour to fortify the argument that tide fluctuation influences the resonant modes, especially the spikes between 20 min and 25 min. The water level at tide gauge station and corresponding spectral density distribution on March 1st, June 1st, September 1st, December 1st in 2013 are demonstrated as Figure 9. On March 1st of 2013, water level was between 1.0 m and 3.2 m; On December 1st of 2013, water level was between 0.5 m and 3.6 m; On June 1st of 2013, water level was between 1.2 m and 3.0 m; On September 1st of 2013, water level was between 1.3 m and 3.1 m. The normal day oscillation contains multiple spikes, and stronger tide fluctuation generates bigger spikes between 20 min and 25 min.

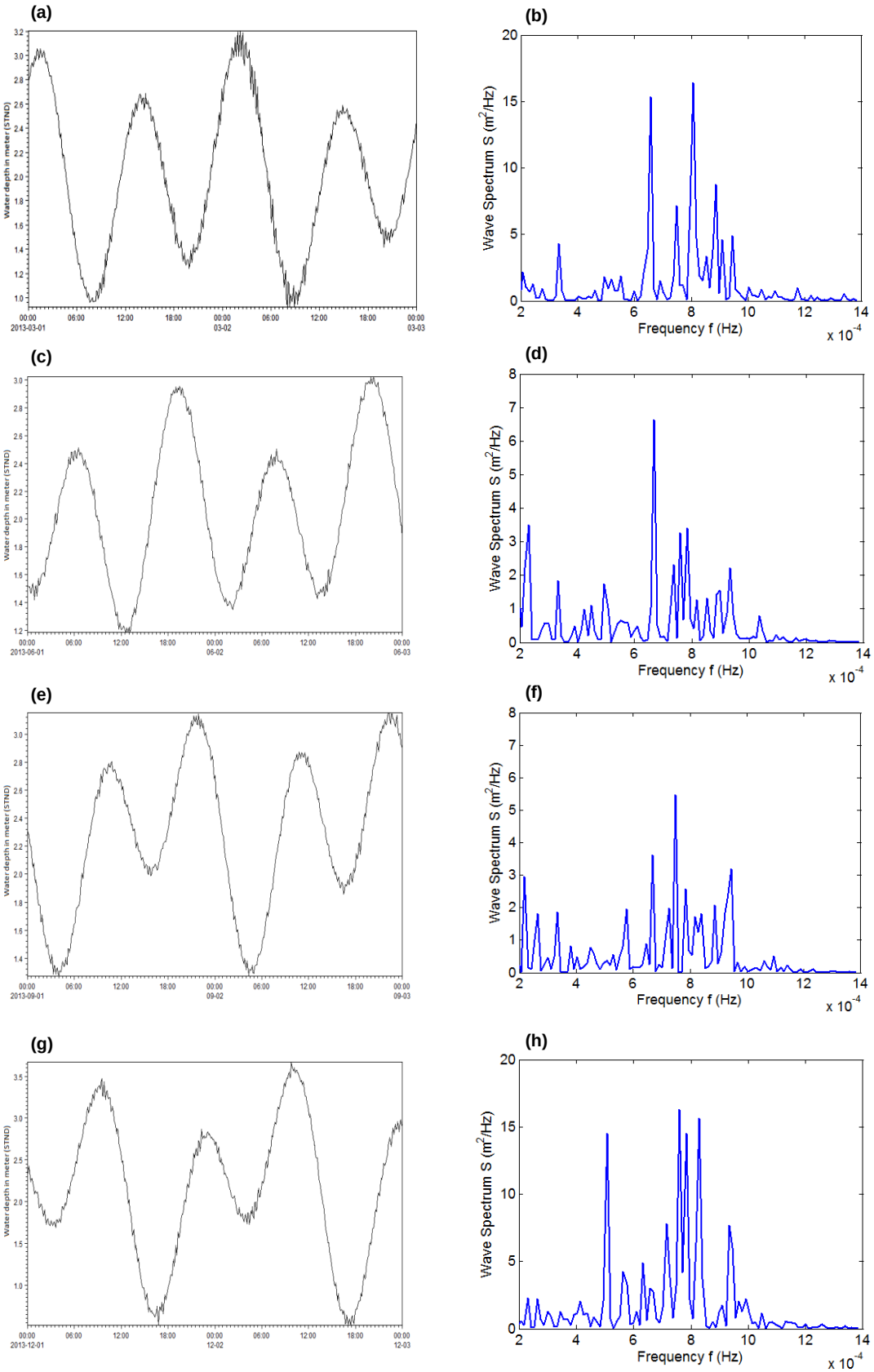

Figure 9. Water level at tide gauge (Station Datum) in Crescent City harbour (a) on March 1st, 2013; (c) on June 1st, 2013; (e) on September 1st, 2013; (g) on December 1st, 2013 (Source: NOAA)
The spectral density distribution with tide filtered (b) on March 1st, 2013; (d) on June 1st, 2013; (f) on September 1st, 2013; (h) on December 1st, 2013

Figure 9 indicates that multiple spikes exist, not only on tsunami events, but also on normal days, which results of energy content of incoming long waves. The moving tide changes the harbour layout and bathymetry, and ultimately demonstrates the resonant modes as variable spikes in the spectrum. The fluctuation of tide level and corresponding change of harbour layout is explicitly associated with the resonant periods between 20 min and 25 min. Therefore, the tide of larger amplitude will generate bigger multiple spikes, especially between 20 min and 25 min in Crescent City harbour.

CONCLUSION

The multiple resonant modes were observed in Crescent City harbour during the tsunami events on Feb. 27th, 2010 and Mar. 11th, 2011. The fluctuating tide level and the corresponding change of harbour layout are the reasons. To ascertain this hypothesis, the numerical wave model based on Boussinesq type equations has been applied into the white-noise analysis of Crescent City harbour.

Through analysis upon different tide levels, the primary resonant mode of Crescent City harbour appears to be multiple spectral spikes. As the water level at the tide gauge rises from 0.8 m to 3.6 m, the fundamental resonant period changes between 20 minutes and 25 minutes. To prove this result in frequency domain, the mild-slope equation is used to simulate the response curves at tide gauge in Crescent City with different tide levels. It remarks 20 minutes at low tide, 22 minutes at mean tide, and 25 minutes at high tide. Study in both time domain and frequency domain demonstrates that tide level and harbour layout influence the primary resonant modes in Crescent City harbour, especially during a long time span of excitement, because the effect of tide level fluctuation and change of harbour layout will have enough time to build up. Additionally, multiple spikes are observed on normal days as the background energy content, and the fluctuation of tide will amplify the resonant spikes between 20 min and 25 min.

In present paper, Boussinesq-type model is used to cross check with the simulation by mild-slope equation, and the consistent results proves that the effect of fluctuating tide level and the corresponding change of harbour layout are the reasons that lead to the multiple spectral spikes in Crescent City harbour.

REFERENCES

Abbott, M.B., H.M. Petersen, and O. Skovgaard. 1978. On the Numerical Modelling of Short Waves in Shallow Water, *Journal of Hydraulic Research*, 16, No. 3, 173-204.

Gierlevsen, T., M. hebsgaard, and J. Kirkegaard. 2001. Wave Disturbance Modelling in Port of Sines, Portugal - with Special Emphasis on Long Period Oscillations, *Proceedings International Conference on Port and maritime R & D and Technology*, Singapore, October 29-13, 2001, 8 pp.

Larsen, J. and H. Dancy. 1983. Open Boundaries in Short Wave Simulations-A New Approach, *Coastal Engineering*, 7, 285-297.

Lee, J.J., X.Y. Xing, and O. Magoon. 2008. Uncovering the Basin Resonance at Crescent City Harbor Region, *Proceedings of ICCE 2008*, Vol. 2, 1210-1222.

Lee, J.J., Z.Y. Huang, Z.Q. Kou and X.Y. Xing. 2012. The Effect of Tide Level on the Tsunami Response of Coastal Harbors, *Coastal Engineering Proceedings*, Vol. 1, No. 33.

Lee, J.J., Z.Y. Huang, and X.Y. Xing. 2013. The Mystery of 2010 Chilean Earthquake Generated Tsunami Waves at Crescent City Harbor, *Coastal Hazards*, 1-12.

Madsen, P.A. 1983. Wave Reflection from A Vertical Permeable Wave Absorber, *Coastal Engineering*, 7, 381-396.

Madsen, P.A., R. Murray, and O.R. Sorensen. 1991. A New Form of the Boussinesq Equations with Improved Linear Dispersion Characteristics, *Coastal Engineering*, Vol. 15, 371-388.

Madsen, P.A., and O.R. Sorensen. 1992. A New Form of the Boussinesq Equations with Improved Linear Dispersion Characteristics. Part 2. A Slowly-varying Bathymetry, *Coastal Engineering*, Vol. 18, 183-204.

Peregrine, D.H. 1967. Long Waves on A Beach, *Journal of Fluid Mechanics*, Vol. 27, Part. 4, 815-827.

Xing, X.Y., J.J. Lee, and F. Raichlen. 2010. Harbor Resonance: A Comparison of Field Measurements to Numerical Results, *Coastal Engineering Proceedings*, Vol.1, No. 32.